Journal of the Technical University of Gabrovo

https://mc04.manuscriptcentral.com/jtug

EFFECT OF COOLING RATE ON THE ATOMIC STRUCTURE OF $Al_{75}Co_{25}$ METALLIC GLASS

Sedat Sengul[1]*, Unal Domekeli[1], Murat Celtek[2]

[1]*Dept. of Physics, Trakya University, 22030, Edirne, Turkey*

[2]*Faculty of Education, Trakya University, 22030, Edirne, Turkey*

ARTICLE INFO

Article history:
Received 30 September 2021
Accepted 25 November 2021

Keywords:
cooling rate, embedded atom method, metallic glass, glass transition temperature, pair analysis

ABSTRACT

In the present study, the effect of cooling rate on the atomic structure and glass formation process of $Al_{75}Co_{25}$ metallic glass was investigated with a series of classical molecular dynamics simulations based on the embedded atom method. The effects of the cooling rate on the atomic structure of the system were discussed in detail using various analysis methods. It has been observed that the cooling rate has a significant effect on the volume and energy of the system, as well as the glass transition temperature is lower in the slower cooled system. We observed a splitting in the second peak of the simulated total (or partial) pair distribution functions, which is a characteristic behavior for metallic glasses. According to the results of the pair analysis method, 1431 and 1541 bonded pairs were the most dominant pairs at high temperatures, and a significant increase was observed in 1551 bonded pairs around the glass transition region with decreasing temperature. We observed that the fraction of them increased when the system was cooled more slowly, indicating that the cooling rate has a significant effect on the formation of the icosahedral order.

INTRODUCTION

Interest in metallic glasses (MG) has grown exponentially since the discovery of the first glassy alloy in 1960 [1]. Because MGs have many unique properties compared to other amorphous materials and conventional metals. These unique properties have brought them to the forefront of materials research and have led them to play key roles in a wide range of applications, such as engineering materials [2, 3]. One of the scientific terminologies for MGs is the glass forming ability (GFA), which describes how easy or how difficult MG formation is [4]. Bulk MG alloys have been extensively studied using traditional solidification methods, and as a result of these studies, many MGs such as Sm-Al-Fe, Y-Al-Cu [5] and Cu-Zr-Ag [6] have been obtained. Among MG materials, Al-based bulk MGs are among the most widely studied materials because they have many unique properties such as good corrosion resistance, low elastic modulus and high specific strength [7, 8]. Intense efforts have been performed to develop Al-based MG materials with improved GFA from past to present, and many new materials have been produced [9, 10]. In addition to experimental studies on Al-based materials, research has also been carried out using molecular dynamics (MD) simulation techniques [11, 12]. Although many studies have been carried out on these materials, their GFA and atomic structure during rapid solidification are still not fully understood. Thus, we focused on the atomic structure of $Al_{75}Co_{25}$ metallic liquid and glass from the Al-based MG family and the cooling rate effect on the glass forming process. In this paper, the evolution of the atomic structure and the glass formation process of $Al_{75}Co_{25}$ binary alloy during the cooling process were investigated by classical MD simulations using the embedded atom method (EAM) potentials. Various methods have been used to characterize the short-range order and describe the local structure of the system. In this process, three different cooling rates (γ=5 K/ps, γ=0.5 K/ps and γ=0.05 K/ps) have been used to observe the effect of the selected cooling rates on the glass formation process. Detailed analyzes of the results obtained from EAM-MD simulations are given in the following sections.

EXPOSITION

The EAM potential developed by Zhou *et al.* [13], which has been reported to give successful results for metals and their alloys, was used to describe the interactions between Al-Al, Co-Co and Al-Co atom pairs. The general form of EAM is as follows;

$$E = \frac{1}{2}\sum_{i,j,i\neq j}\phi_{ij}(r_{ij}) + \sum_{i}F_i(\rho_i) \quad (1)$$

where ϕ_{ij} is the pair potential between atoms i and j. F_i is the embedding energy and ρ_i electron density is given as,

$$\rho_i = \sum_{i,j,i\neq j} f_j(r_{ij}) \quad (2)$$

* Corresponding author. E-mail: sesedatse@gmail.com

The functional form of the pair potential between atoms of the same type is given below;

$$\phi(r)=\frac{A\exp\left\{-\alpha\left(\frac{r}{r_e}-1\right)\right\}}{1+\left(\frac{r}{r_e}-k\right)^{20}}-\frac{B\exp\left\{-\beta\left(\frac{r}{r_e}-1\right)\right\}}{1+\left(\frac{r}{r_e}-\lambda\right)^{20}} \quad (3)$$

where A, B, α and β are four different adjustable parameters. r_e is the equilibrium distance between the nearest neighbors. κ and λ are the cutting parameters. The electron density function given in Equation 4 is very similar to the second part of the pair potential given in Equation 3, with the only difference being that f_e is used instead of parameter B:

$$\rho(r)=\frac{f_e\exp\left\{-\beta\left(\frac{r}{r_e}-1\right)\right\}}{1+\left(\frac{r}{r_e}-\lambda\right)^{20}} \quad (4)$$

The pair potential between Al and Co species has been determined using the following relation.

$$\phi_{Al,Co}(r)=\frac{1}{2}\left[\frac{\rho_{Al}}{\rho_{Co}}\phi_{Al,Al}(r)+\frac{\rho_{Co}}{\rho_{Al}}\phi_{Co,Co}(r)\right] \quad (5)$$

By fitting the embedded energy function in three different electron density ranges, it is expressed as a piecewise function as

$$F(\rho)=\begin{cases}\sum_{i=0}^{3}F_{ni}\left(\frac{\rho}{\rho_n}-1\right)^i, \rho<\rho_n, \rho_n=0.85\rho_e\\ \sum_{i=0}^{3}F_i\left(\frac{\rho}{\rho_e}-1\right)^i, \rho_n\le\rho<\rho_0, \rho_0=1.15\rho_e\\ F_e\left[1-\ln\left(\frac{\rho}{\rho_s}\right)^{\eta}\right]\left(\frac{\rho}{\rho_s}\right)^{\eta}, \rho_0\le\rho\end{cases} \quad (6)$$

EAM potential parameters for pure Al [14] and Co [15] were taken from Ref [13]. The open source code, DL_POLY 2.0 package, was used to perform the atomic simulations [16]. The simulations were carried out within the constraints of isobaric-isothermal ensemble (NPT) under zero external pressure. In simulations, pressure and temperature were kept under control using Berendsen barostat and thermostat. Newtonian equations of motion were solved by Verlet leapfrog algorithm with a time step of 1 fs. The initial configuration was the fcc unit cell which is periodic in the directions of X-, Y- and Z- of Cartesian coordinates. The total number of atoms was 5324 (3993 Al and 1331 Co atoms). Before applying the heating procedure, the system was first heated from 0 K to 300 K, and then cooled from 300 K to 0 K again, to relieve stress on the system, which was set up in a perfect fcc crystal structure at 0 K. Then, the system was heated to 2000 K by temperature increments of 50 K, which is sufficiently higher than the melting point of the $Al_{75}Co_{25}$ alloy. To obtain a well-equilibrated liquid, the system was run for another 500,000 timesteps at 2000 K. The cooling procedure was carried out by reducing the temperature from 2000 K to 300 K at 50 K intervals using three different cooling rates (γ=5 K/ps, γ=0.5 K/ps and γ=0.05 K/ps). Snapshots of the simulation box showing the atomic distributions at different temperatures (300, 1000 and 1500 K) during the heating (with γ=5 K/ps heating rate) and cooling (with γ=0.05 K/ps cooling rate) processes are shown in Fig. 1.

While the atomic arrangement at 300 K shows a distribution peculiar to crystal-like structures during the heating process, when the temperature is increased to 1000 K, it is now seen that the atoms exhibit a random distribution in some regions besides the crystal-like arrangement. When the temperature finally reaches 1500 K, the atoms in the system show a random distribution, which is clear evidence that the system has transitioned from the solid phase to the liquid phase. These findings are also supported by the energy-temperature (E-T) and volume-temperature (V-T) curves shown in Figs. 2(a) and 2(b). On the other hand, in each of the snapshots of the cooling process at different temperatures, it seems that the atoms exhibit a random distribution, just like in liquid structures. This is attributed to the fact that crystal nucleation is prevented even at the slowest cooling rate in the system, and as a result, the system solidifies in an amorphous structure. This will be supported by different analyzes in the following sections. One of the most important thermodynamic properties of MGs is the glass transition temperature (Tg). Tg can be determined from E-T, V-T or Wendth-Abraham parameter-temperature (WA-T) curves. In this study, Tg's for all three cooling rates were determined from the WA parameter temperature (MWA-T) curve modified by Celtek et al. [17].

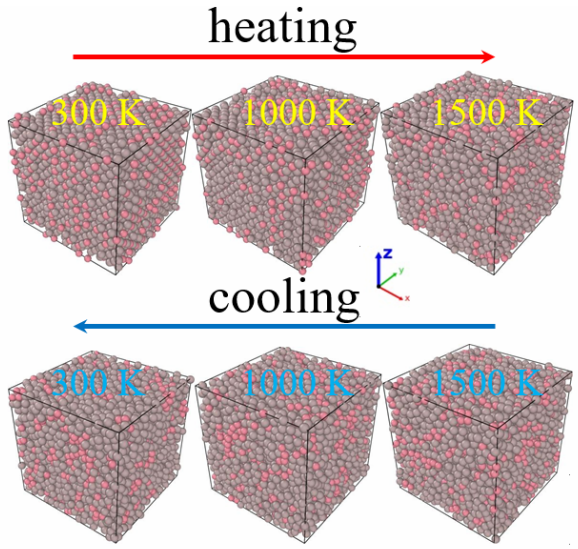

Fig. 1. Snapshots of simulation box at 300, 1000, and 1500 K during the heating and cooling process. The gray and pink balls represent Al and Co atoms, respectively.

As can be seen from the E-T and V-T curves given in Figs. 2(a) and 2(b), a linear increase is observed between 300 K and 1000 K during the heating process, while a sudden and sharp increase is observed at 1000 K. The temperature at which this sudden increase starts corresponds to the melting point where the crystal and liquid phase are together. Then, the heating curves continue to increase linearly with a different angle of slope starting from 1050 K towards higher temperatures, indicating that the system is now in equilibrium in liquid form. The

cooling curves and the heating curves almost overlap at high temperatures, and there is a slight difference in the slopes of the cooling curves between decreasing temperature and 800-300 K, indicating that the system has transitioned from liquid to amorphous structure. The curves in these temperature ranges are enlarged and shown in the inset of the figures in order to realize the difference due to the cooling rate more clearly. The pair distribution function, g(r), is very often used for the atomic characterization of solid, liquid and amorphous structures. In our study, the partial g(r) ($g_{ij}(r)$) of the $Al_{75}Co_{25}$ system for the α and β atom types is defined as

$$g_{\alpha\beta}(r) = \frac{V}{N_\alpha N_\beta}\left\langle \sum_{i=1}^{N_\alpha} \frac{n_{i\beta}(r)}{4\pi r^2 \Delta r} \right\rangle \quad (7)$$

where V represents the total volume of the system, and N_α and N_β represent the number of α and β atoms, respectively. The total *g(r)*'s calculated for various temperatures during the heating and cooling process (with γ=5 K/ps heating and cooling rate) are shown in Fig. 3.

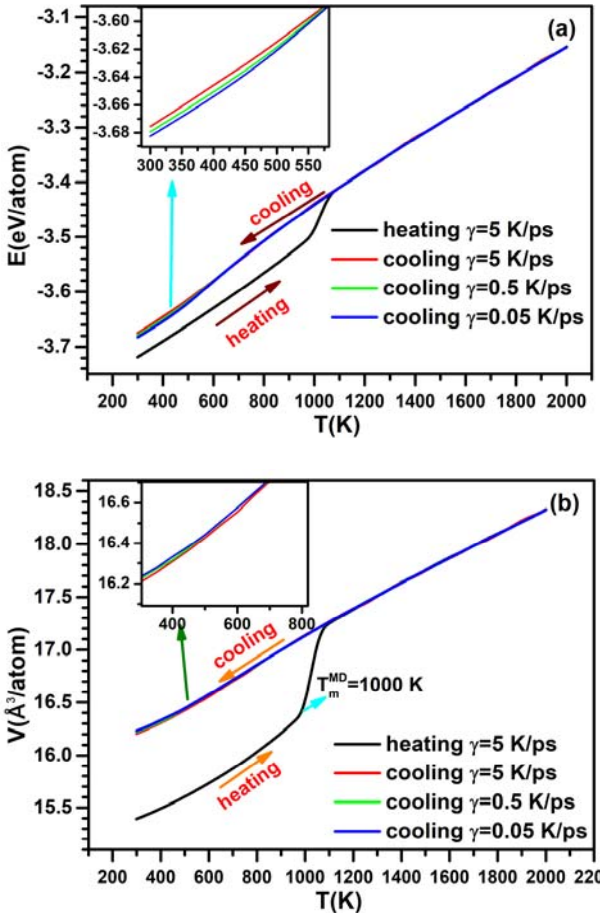

Fig. 2. (a) E-T and (b) V-T curves obtained during the heating and cooling process

Both g(r)s obtained from heating and cooling at 1500 K overlap each other, indicating a liquid that is equilibrated at the same temperature. At 1000 K, while the peaks of g(r) obtained from cooling exhibit the same behavior of liquid structures, on the other hand, a hump appears around the first minimum of g(r) obtained from heating and the main peaks are more prominent. This is related to the coexistence of the solid and liquid phase at this temperature, as discussed above, that is, this temperature corresponds the point at which the melting process of the system begins. Finally, at 300 K, the g(r) of the heating process exhibits very sharp and typical peaks reflecting the characteristic of fcc crystal structure, while a clear splitting occurs at the second peak of the g(r) of the cooling process. This splitting behavior is typical for MGs, the same splitting is observed for other cooling rates, but not shown here to avoid duplication. The $g_{ij}(r)$'s of Al-Al, Co-Co and Al-Co pairs calculated at 300 K using three different cooling rates are plotted together in Fig. 4. The second peaks of all gij(r)s have the same splitting as the total g(r)s, but with a much more pronounced splitting. This splitting is attributed to the short-range order (SRO) and the medium-range order (MRO), which begin to occur in the system during cooling and subsequently develop. In addition, the $g_{ij}(r)$ obtained from all cooling rates are almost the same, which indicates the stability of the system in the glassy structure. The inset shows a zoomed-in form of the first peaks of $g_{ij}(r)$ for the Co-Co pair.

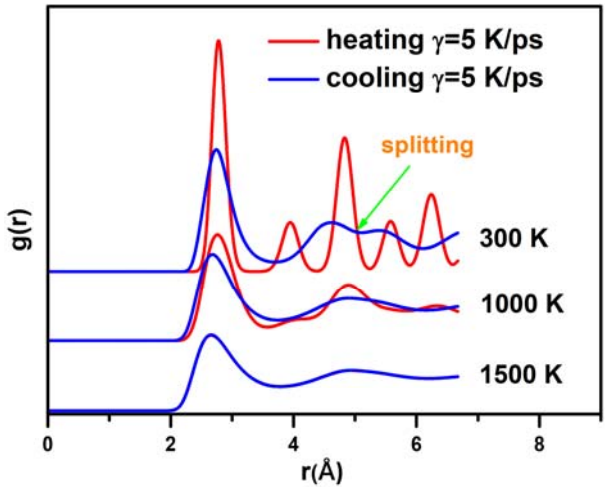

Fig. 3. g(r) curves obtained at different temperatures during the heating and cooling process

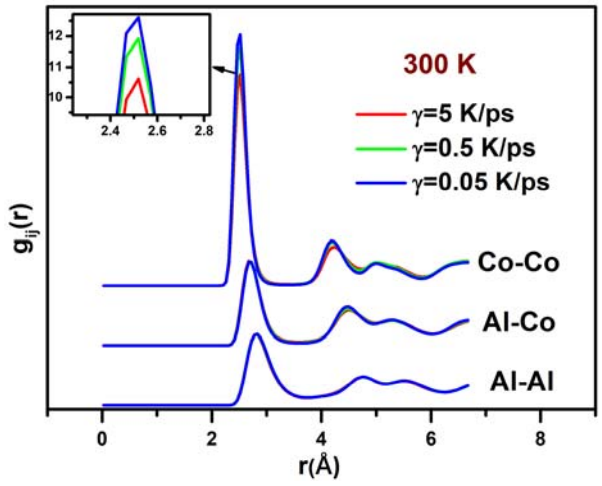

Fig. 4. $g_{ij}(r)$ curves of Al-Al, Co-Co, and Al-Co pairs calculated at 300 K using three different cooling rates

Fig. 5 depicts the variation of the MWA parameter with temperature for a cooling rate of γ=0.05K/ps. The T_g was determined from the intersection point of the linear fit lines drawn to the low and high-temperature ranges of the MWA curve. T_g values for γ=5 K/ps, γ=0.5 K/ps and γ=0.05 K/ps cooling rates have been determined as 565 K, 545 K and 530 K, respectively. These results show that the T_g values

decrease accordingly when the system is cooled more slowly.

The pair analysis technique proposed by Honeycutt and Andersen (HA) has been used to examine the evolution of the system's microstructure during the cooling process [18]. The temperature-dependent evolution of the most dominant bonded pairs in the system according to the HA results for a cooling rate of γ=0.05 K/ps is shown in Fig. 6. For high temperatures, the most dominant pairs are the 1431 and 1541 bonded pairs, which represent the distorted icosahedra (deficos). While the fraction of 1551, 1541, and 1661 bonded pairs increases with decreasing temperature, the fraction of other bonded pairs (1311, 1321, 1421, 1422, 1441 and 1661) starts to decrease around 900 K. Especially in the fraction of 1551 bonded pairs representing the ideal icosahedra (icos) order among them, a very significant increase is observed from 14.9% at 2000 K to 40.82% at 300 K. The predominance of icos and deficos types at low temperatures indicates that the icosahedral order is dominant due to more favorable energy. The fractions of all these bonded pairs depending on the cooling rate at 300 K are shown in Fig. 7. Again, for all cooling rates, it is seen that the most dominant bonded pairs are icos+deficos types, and among these, icos types increase depending on the decreasing cooling rate. No significant change was observed in the fraction of fcc+hcp, bcc, and other types depending on the cooling rate. This shows us that the system is stable in glassy structure at all cooling rates and deficos types turn into icos types depending on the decreasing cooling rate.

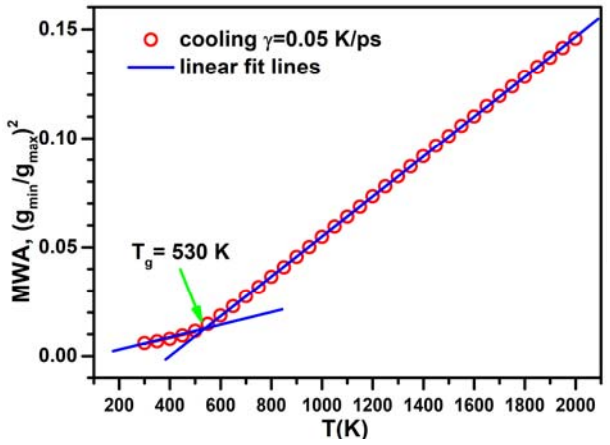

Fig. 5. Temperature-dependent evolution of the MWA parameter for a cooling rate of γ=0.05 K/ps

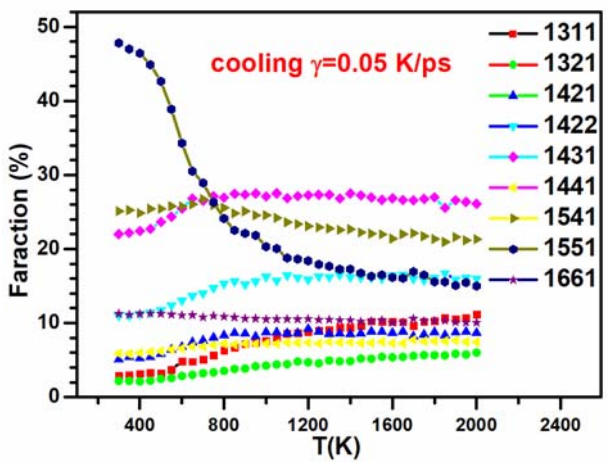

Fig. 6. Fraction of most dominant HA bonded pairs for a cooling rate of γ=0.05 K/ps as a function of temperature

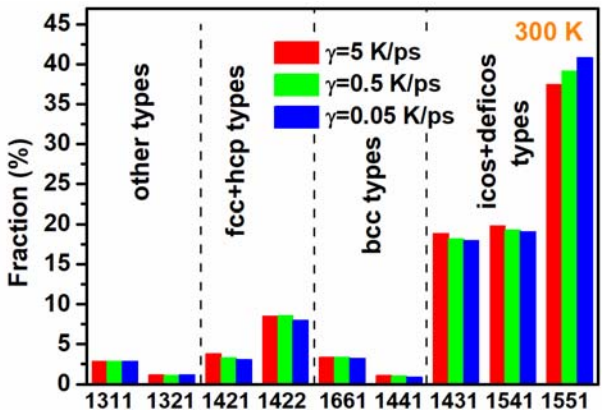

Fig. 7. Fraction of most common bonded pairs at 300 K for three different cooling rates

CONCLUSION

In this study, the effect of cooling rate on the atomic structure of and the glass forming process of $Al_{75}Co_{25}$ alloy was investigated by MD simulations using the EAM potential. A splitting, typical for glassy structures, is observed in the second peaks of the g(r) (or $g_{ij}(r)$) curves calculated at low temperatures. It has been observed that the Tg decreases depending on the slower the system is cooled. According to the HA analysis results, it was seen that the most dominant types were icos+deficos types at all temperatures for three different cooling rates. As a result, no first-order phase transition was observed in the structure of the system for all cooling rates during the cooling process and it was observed that the system was stable in the glassy structure.

REFERENCES

[1] Klement W., Willens R.H., Duwez P. Non-crystalline Structure in Solidified Gold–Silicon Alloys. Nature 187 (1960) 869–870

[2] Inoue A., Takeuchi A. Recent development and application products of bulk glassy alloys. Acta Mater 59 (2011) 2243–2267

[3] Axinte E. Metallic glasses from “alchemy” to pure science: Present and future of design, processing and applications of glassy metals. Mater Des 35 (2012) 518–556

[4] Inoue A. Stabilization of metallic supercooled liquid and bulk amorphous alloys. Acta Mater 48 (2000) 279–306

[5] Fan G. Glass-forming ability of RE–Al–TM alloys (RE=Sm, Y; TM=Fe, Co, Cu). Acta Mater 48 (2000) 3823–3831

[6] Song K.K., Gargarella P., Pauly S. et al. Correlation between glass-forming ability, thermal stability, and crystallization kinetics of Cu-Zr-Ag metallic glasses. J Appl Phys 112 (2012) 063503

[7] Guan P., Chen M., Egami T. Stress-Temperature Scaling for Steady-State Flow in Metallic Glasses. Phys Rev Lett 104 (2010) 205701

[8] Yang B.J., Yao J.H., Zhang J. et al. Al-rich bulk metallic glasses with plasticity and ultrahigh specific strength. Scr Mater 61 (2009) 423–426

[9] Louzguine-Luzgin D.V., Seki I., Yamamoto T. et al. Double-stage glass transition in a metallic glass. Phys Rev B 81 (2010) 144202

[10] Park E.S., Jeong E.Y., Lee J-K. et al. In situ formation of two glassy phases in the Nd–Zr–Al–Co alloy system. Scr Mater 56 (2007) 197–200

[11] Liu C., Wang F., Rao F. et al. Glass-forming ability of Al-Co alloy under rapid annealing. J Appl Phys 113 (2013) 154306

[12] Kbirou M., Mazroui M, Hasnaoui A. Atomic packing and fractal behavior of Al-Co metallic glasses. J Alloys Compd 735 (2018) 464–472

[13] Zhou X.W., Johnson R.A., Wadley H.N.G. Misfit-energy-increasing dislocations in vapor-deposited CoFe/NiFe multilayers. Phys Rev B 69 (2004) 144113

[14] Celtek M., Sengul S., Domekeli U. The Evolution of Atomic Structure of the Zr48Cu36Ag8Al8 Bulk Metallic Glass in the Rapid Cooling Process. Süleyman Demirel Univ J Nat Appl Sci 23 (2019) 954–962

[15] Celtek M., Sengul S. Effects of cooling rate on the atomic structure and glass formation process of Co90Zr10 metallic glass investigated by molecular dynamics simulations. Turkish J Phys 43 (2019) 11–25

[16] Smith W., Forester T.R.. DL_POLY_2.0: A general-purpose parallel molecular dynamics simulation package. J Mol Graph 14 (1996) 136–141

[17] Celtek M., Sengul S., Domekeli U. et al. Dynamical and structural properties of metallic liquid and glass Zr48Cu36Ag8Al8 alloy studied by molecular dynamics simulation. J Non Cryst Solids 566 (2021) 120890

[18] Honeycutt J.D., Andersen H.C. Molecular Dynamics Study of Melting and Freezing of Small Lennard- Jones Clusters. J Phys Chem 91 (1987) 4950–4963